Hydroxide Impurity in Ice[†]

Lukasz Cwiklik,*[,‡] J. P. Devlin,[§] and Victoria Buch[‡]

The Fritz Haber Institute for Molecular Dynamics, The Hebrew University, Jerusalem 91904, Israel, and Department of Chemistry, Oklahoma State University, Stillwater, Oklahoma 74078

Received: January 19, 2009; Revised Manuscript Received: March 15, 2009

The role of hydroxide ions in proton mobility in water ice I is studied using both computational methods and isotopic exchange experiments. A strong influence of base adsorbate at the ice nanoparticle surface on proton activity is observed experimentally. Trace doping of the ice surface with base adsorbates stops proton activity, whereas the activity is restarted if larger amounts of adsorbate are present. On the basis of density functional theory calculations for ice slabs, these observations are rationalized by the existence of traps strongly binding hydroxide ions both at the surface and in the ice interior. These strongly binding sites stop proton mobility by immobilization of hydroxide ions; however, in the presence of an abundance of OH^-, the deepest traps are saturated and thus the proton activity is restored. A rather broad energy distribution is calculated for the hydroxide located at different lattice sites.

I. Introduction

To account for electrical transport properties of water ice, the presence of hydronium and hydroxide ionic defects was postulated in the tetrahedral ice structure.[1] In pure ice these ionic defects originate, like in liquid water, from autoionization reaction of water molecules. In ice, ionic defects are accompanied by Bjerrum orientational defects, corresponding to misaligned water molecules in the tetrahedral H-bond network; Bjerrum defects promote rotational mobility.[2] The presence of both types of defects was found to be responsible for the protonic semiconductivity of ice. The tetrahedral ice structure formed by oxygen atoms of water molecules exhibits a protonic disorder. That is, hydrogen atoms do not form a periodic structure; rather, the orientations of water molecules are quasi-random within a constraint of completeness of the tetrahedral H-bond network. Charge flow occurs by proton transfer between an ion (hydronium or hydroxide) and a neighboring water molecule, which thus becomes an ion. After passage of a proton, its path becomes blocked for motion of an additional proton, until orientational relaxation takes place via Bjerrum defect activity (Bjerrum defects are also considered as charge carriers due to the polarity of H_2O.)[1] Thus, protonic semiconductivity requires movement of both ionic and orientational defects, and both defect types must be taken into consideration for understanding electric transport processes in ice. It should also be noted that the lack of full periodicity is an important issue in computational studies of ice Ih, because different possible proton arrangements should be considered in computational treatment of ice.

The defects in ice not only may originate from autoionization or rotational movements of water molecules, but also can be induced by the presence of impurities.[1] Experiments on ice nanoparticles demonstrated a key role of the ice surface in controlling the presence and the mobility of defects in the interior of ice. That is, molecules adsorbed at the surface of ice can affect dramatically the behavior of the defects in the bulk.[3,4] Even more interesting from the chemical point of view is the fact that the opposite interactions are also possible. Namely, one can glean information from defect activity on the chemical state of the adsorbate, as was shown recently for ionization of sulfur dioxide at the ice surface.[5]

In the computational part of this work we focus on the properties of the hydroxide ions in ice. Preliminary results were reported in a preceding letter, where a new possible structure for OH^- in the interior of ice was proposed.[6] That new configuration, where OH^- accepts four hydrogen bonds and the OH^- axis points into a cavity in the crystal structure, was shown to trap hydroxide and thus to reduce the proton migration rate. That "off-the-lattice" configuration was compared to the usually assumed "in-the-lattice" bulk configuration in which OH^- accepts three hydrogen bonds and donates one to neighboring water molecules. Here, extended discussion is given of the binding sites in the ice interior. In addition, the ice surface is taken into account, and we consider the problem of surface versus bulk energetics of the hydroxide. Similarly to the interior case, we are looking for energetically preferred configurations for OH^-. The computational study employs density functional theory (DFT). The calculations were carried out on a three-bilayer ice slab. The main computational tool was Quickstep, a Gaussian and plane waves based (GPW) ab initio code which is a part of the CP2K package,[7,8] and which enables structure minimizations and molecular dynamics simulations with periodic boundary conditions.

A related study was recently pursued by Knight and Singer on OH^- energetics within bulk ice.[9] Their bulk model included an orientational L-defect in addition to the hydroxide in the in-the-lattice configuration. The influence of orientational structure on the system energetics was considered. The results are relevant to base catalysis of the orientational ordering transition at 72 K.

Hydroxide structure and dynamics in the case of liquid water were recently addressed in the literature. Tuckerman, Chandra, and Marx demonstrated computationally that, in the liquid, the hydroxide acquires a hypercoordinated solvation shell from which it accepts four hydrogen bonds; this configuration inhibits

[†] Part of the "Robert Benny Gerber Festschrift".

* To whom correspondence should be addressed. E-mail: lukasz@fh.huji.ac.il.

[‡] The Hebrew University.

[§] Oklahoma State University.

10.1021/jp900545d CCC: $40.75
Published on Web 04/15/2009

proton jumps.[10] These findings were confirmed by both X-ray diffraction and X-ray photoelectron spectroscopy measurements.[11,12] The problem of surface vs bulk preference of hydroxide in liquid water was also studied both computationally and experimentally. It was shown that hydroxide in liquid systems does not display a pronounced surface preference,[13,14] and this theoretically predicted picture is supported by recent surface-selected spectroscopic measurements.[15] However, these observations are in a contradiction with the interpretation of macroscopic measurements performed for bubble and droplet systems; therefore, the surface preference of OH^- in water is a source of controversy.[16,17]

The present computational studies will be used to interpret experimental data on defect activity in ice nanocrystals, as reflected by isotopic exchange experiments. In the past, methods have been developed that allow the isolation of intact D_2O molecules at the lattice and surface sites of ice films[18] and ice nanocrystals[13] at temperatures below ~140 K. The infrared spectra of such isolated D_2O molecules represent a versatile probe of both ionic and orientational defect activity in the interior and at the surface of ice. When a proton, moving along the H-bonded "wires" in ice, passes through an isolated D_2O molecule, the reaction

$$D_2O + H_2O \rightarrow 2HDO$$

takes place. The resulting HDO units are connected by a deuterium bond so that, in the interior of ice, the two tandem O−D bonds of the HDO units are strongly coupled by the dynamic dipole−dipole coupling. The latter coupling is reflected by a unique vibrational-mode doublet with components near 2445 and 2390 cm^{-1}. If defect motion in ice were limited to that of ions, the complete spectroscopic pattern for isotopic exchange would appear as the partial replacement of the D_2O symmetric and asymmetric stretch doublet (2450 and 2365 cm^{-1}) by this new $[HDO]_2$ doublet;[19] any further isotopic separation would be stymied as proton jumps can move a deuterium only from one end of the hydrogen bond to the other.

However, FTIR spectra show that the separation of the HDO units can proceed until isotopic scrambling is complete. This continuation can be explained by invoking the activity of the Bjerrum orientational defects. Orientational motion can remove the deuterium atoms from their original H-bond so that the "random" sequence of passage of ionic and orientational defects leads to complete scrambling of the isotopes. The resulting isolated HDO units also have a characteristic spectrum with a single O−D stretch band near 2420 cm^{-1} that denotes the progressive scrambling. Thus, the evolution of the spectrum from one unique doublet (corresponding to D_2O) to another (corresponding to $(HDO)_2$ with two OD groups in tandem), and then eventually to a single band (isotopically isolated HDO), allows quantitative measure of both the ionic and the orientational defect activities.[18]

Isotopic exchange of isolated D_2O molecules also provides a quantitative probe of ionic defect activity at the ice *surface*. Fortuitously, the infrared absorption bands of the O−D stretch modes of the free O−D surface bonds of D_2O and HDO are spaced by 14 cm^{-1}, appearing at 2726 and 2712 cm^{-1}, respectively (see Figure 7 in section III). The loss of D_2O band intensity with time offers a quantitative measure of the rate of proton passage through the surface D_2O molecules.[4] The corresponding growth of the HDO band is also indicative of this activity, but is not quantitative as the new HDO molecules also adjust, in a manner dependent on the temperature, to a known preference for D vs H bonding to the "subsurface" ice.[20]

Historically, the isotopic measurements noted above have usually been applied to determination of the excess proton activity, rather than to that of the hydroxide ion, which is of particular interest here. This followed from a much greater protonic than hydroxide activity in pure ice. Observations on thick ice films indicated that protonic activity near 145 K is sufficient for ion passage through 50% of the ice lattice sites on a 1/2 h time scale.[18] Similar but somewhat greater defect activity has been noted for the core ice of nanocrystals.[3] These studies also showed that isotopic exchange in ice can be stopped by trace doping with ammonia, apparently through shifting of the autoionization equilibrium mentioned earlier. Elimination of protons through a progressive increase in base dopant was found to first stop and then restart the exchange process, suggesting orders of magnitude less mobility for the hydroxide ion but sufficient OH^- activity to be significant when the hydroxide ion concentration is increased greatly.

Recent isotopic exchange data for ice nanocrystals have indicated that both the protonic (hop) and the Bjerrum (turn) steps for pure ice are enhanced near the surface, with the surface proton activity greater than for the core ice by more than an order of magnitude.[13] This observation is consistent with reports based on reactive ion scattering measurements on thin film ice samples that indicated greater proton defect activity at the surface than within the interior of thin film ice samples.[21] In fact, observations on the influence of adsorbates on the core exchange rates have led to the conclusion that, below 150 K, interior defect activity merely reflects the surface autoionization equilibrium.[4] That is, the ice−surface equilibrium is the source of an occasional ion defect that overcomes an activation barrier to penetrate to the ice core. This concept is affirmed by (a) an ability to control the interior activity by adsorbates and (b) the impossibility of the weak interior ionic defect activity at 136 K to achieve equilibrium on the observational time scales, whereas the response of both the surface and interior rates to adsorbates is effectively instantaneous.

In the experimental part of this paper the focus is on the behavior of the hydroxide ion at the surface and in the interior of ice nanocrystals, particularly as observed for varying levels of base adsorbate. Data will be considered for two similar bases, ammonia and the stronger proton acceptor monomethylamine (MMA), with the adsorbate effect on the isotopic exchange judged through comparison with results for pure ice particles.

In section II, computational and experimental methods are addressed. In section III, the results are described for both approaches. Discussion and conclusions are presented in section IV.

II. Methods

Computational Methods. As shown in experiments,[4] surface processes strongly influence the behavior of defects in the bulk of ice, and hence, to describe the behavior of hydroxide in ice, one needs to account for the presence of the surface. In simulations we employed an ice slab model with two open surfaces as presented in Figure 1. The model consisted of three bilayers of ice Ih, with 24 water molecules in each bilayer. The surfaces corresponded to the basal planes of the hexagonal ice structure. The inner ice bilayer contains only four-coordinated water molecules, while in each of the external bilayers half of the molecules are three-coordinated and contain either a dangling H or a dangling O. A free surface of ice in a low-temperature regime may either exhibit proton disorder or form a more ordered, so-called Fletcher, phase with the energy preference toward the Fletcher one.[22,23] At the disordered surface dangling hydrogens of water molecules are located randomly, whereas at the Fletcher phase surface water molecules form alternating

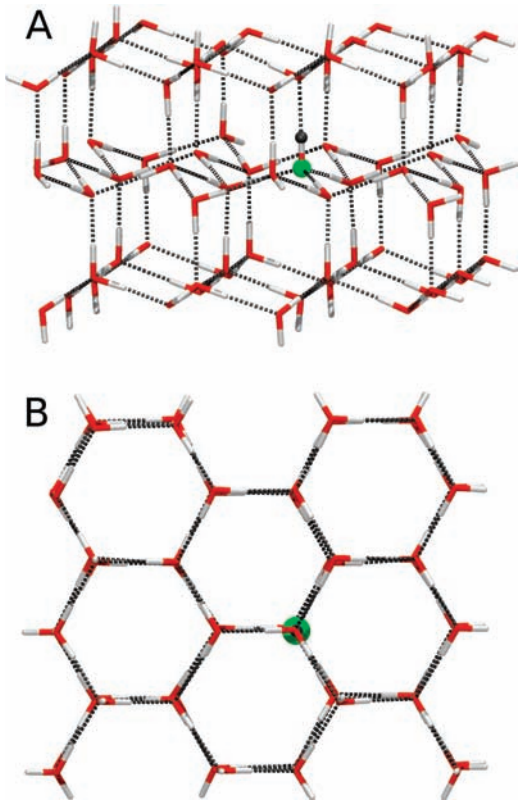

Figure 1. A typical slab of 71 water molecules and one hydroxide used in the calculations (A, side view; B, top view). Color coding: red, oxygen atoms of water molecules; white, hydrogen atoms of water; green, oxygen of hydroxide; gray, hydrogen atom of hydroxide. Gray dotted lines represent hydrogen bonds.

rows with dangling hydrogens and dangling oxygens. We took into account both limits, allowing one of the slab's surfaces to be the Fletcher type and the other to be a proton-disordered one (see Figure 1, top). (There is also an option for partial ordering of the dangling-atom pattern[23,24] which is, however, not considered due to the limited size of the model.) Otherwise, the water molecules were orientationally disordered within the constraints of completeness of the H-bond network. The scheme to generate orientationally disordered ice models is described in ref 25.

Two-dimensional periodic boundary conditions were applied in the directions parallel to the surfaces, and the periodic box size was equal to 13.5×15.6 A^2. To study the behavior of hydroxide in ice, 1 of the 72 water molecules was replaced with OH^-. The OH^- ion was generated by (a) removing one of the surface dangling-H atoms in the disordered surface and (b) performing a sequence of geometric transformations corresponding to proton transfer to OH^- from a neighboring water molecule; as a result of these transformations, the hydroxide ion is displaced to a desired position within the ice lattice. A series of minimizations of the total energy of the slab with respect to the positions of all atoms were then performed for varying the position of OH^- in the system. Configurations with OH^- at each possible lattice location were probed. The above scheme to generate a OH^--containing lattice model is not unique. It was chosen since it results in a complete H-bond network and preservation, for the different structures, of the dangling-atom pattern at the surface; the latter is known to affect significantly the slab energetics.[22−24,26] It was of interest to avoid significant variations in the dangling-atom pattern to focus on the influence of the hydroxide ion on the slab energetics. Different OH^- positions were examined since the energetics is affected by the local orientational structure of ice in the vicinity of the hydroxide.

We also probed an additional family of OH^--containing structures in which OH^- accepts four H-bonds, while the unbonded hydrogen points toward a cavity in the ice structure. Initial results on this off-the lattice hydroxide configuration were reported in a previous study.[6] The new configuration can be considered as a recombination product of an in-the-lattice OH^- configuration described above and a D-defect.[1] An off-the lattice configuration was generated from an in-the-lattice one by rotating a water molecule in the vicinity of in-the-lattice OH^-, so that an L- and a D-defect pair was generated. That is, a water molecule accepting initially a H-bond from OH^- was rotated so that one of the water OH bonds was pointing toward the hydroxide in a OH^-−HOH pattern (a classical model for a D-defect);[1] OH^- was then rotated away from the O···O axis to point into a neighboring cavity to reduce the electrostatic repulsion. The associated L-defect (in which a OH-bond is missing from the near-neighbor O···O axis between two water molecules) was subjected to a series of geometric transformations which displaced it within the lattice, until the L-defect was found at the surface, in the vicinity of a dangling-OH bond of a three-coordinated surface water molecule. The latter water molecule was finally rotated so that the initially dangling OH was used to "heal" the L-defect. The resulting structure was minimized with respect to coordinates of all atoms. (Note that the process of generation of off-the-lattice minima alters the dangling-H pattern at the surface, because of the recombination between an L-defect and a dangling OH.)

In the present study, calculation of off-the-lattice minima is attempted at each lattice site. The resulting minimum energies are compared to those corresponding to in-the-lattice configurations.

The corresponding minimum-energy structures are displayed and further discussed in the Results. It was shown in the preliminary study[6] that the resulting minimized off-the-lattice configurations may have lower energies than the corresponding in-the-lattice ones.

The electronic structure of the slabs was studied using periodic DFT. The CP2K/Quickstep code which combines mixed Gaussian basis and plane-wave basis (GPW)[7,8] was employed. The BLYP functional[27,28] with the DZVP basis set and GTH-type pseudopotential[29] were used. The energy cutoff for plane waves was equal to 280 Ry. We also performed test calculations with expanded basis sets (triple-ζ type and cutoff values up to 400 Ry).

Experimental Methods. As noted in section I, the observation of defect activity in ice depends on the ability to quantitatively monitor the FTIR absorbance spectra of the isolated isotopomers (D_2O, $[HDO]_2$, and HDO) for either H_2O ice films[18] or nanocrystals.[13] With the surface recognized as the probable source of the interior defect activity, the focus here is on ice nanocrystals of a size such that 5−10% of the water molecules of a sample (i.e., 30−15 nm in diameter) reside there. Such nanocrystals, as routinely studied,[30] have been prepared by pulsing ∼1% mixtures of water, in either nitrogen or helium gas, into a cold condensation cell to pressures of 100− 400 Torr at temperatures of 70−120 K. The crystal size is determined primarily by a combination of the percentage of water in the gas mixtures and the temperature of the condensation cell. The nanocrystals can be sampled as aerosols or allowed to form arrays, since a small fraction of the aerosol particles quickly assemble on the infrared windows of the cell. The array

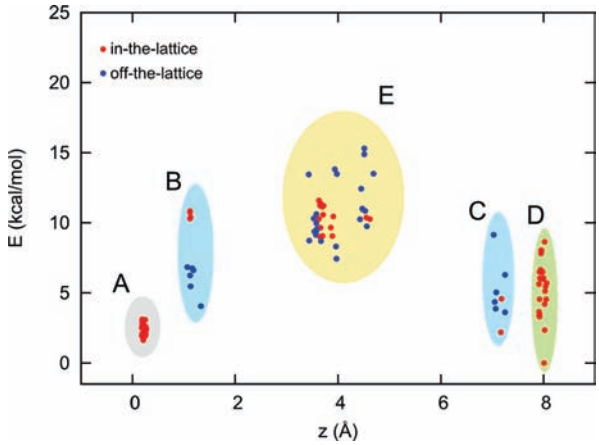

Figure 2. Energy values of optimized slabs as a function of the position of the oxygen atom in OH^- along the z-axis of the slab. Zero energy was set at the lowest energy structure. The points in groups A and B represent minimizations with OH^- at the Fletcher-type surface, those in groups C and D minimizations with OH^- at the proton-disordered surface, and those in group E minimizations with OH^- in the interior bilayer. Red and blue points correspond to OH^- in in-the-lattice and off-the-lattice configurations, respectively. Further details are given in the text.

method provides a stable sample the optical thickness of which can be optimized for a given experiment through a choice of the number of load−pump cycles and for which isotopic exchange observations can be extended over many hours and a sizable temperature range.

The isolation of D_2O within the H_2O nanocrystals requires that a dilute amount of D_2O, in a separate gas mixture of the same pressure, enters the cold condensation cell at the same time and space as the H_2O pulse. This is accomplished by loading through coaxial tubing with both pulses initiated simultaneously using a double-bore valve; see Figure 7 of ref 14. For exchange rate studies within the core of the ice nanocrystals, vibrational decoupling of the D-isotopomers was assured by using ~0.03% D_2O in the gas mixtures. Since the vibrational modes of the free O−D surface groups have dipole strengths much less than in the H-bonded interior, vibrational coupling of the dangling-O−D groups is not a factor in the spectra. Therefore, though satisfactory surface and core data were commonly obtained for the same sample, D_2O/H_2O ratios of ~0.1 were sometimes used to compensate for the weak surface-dangling-bond band intensities.

The base molecules, ammonia or monomethylamine, can be dosed onto the nanocrystals of an array by vapor diffusion, but superior control and uniformity of doping is obtained by mixing small dopant particles within the ice arrays by alternating the pulses of water with dopant gas mixtures. Warming of the arrays for measurement of exchange rates is then accompanied by transfer of the more volatile dopants to the ice particle surfaces. For aerosol samples, surface dosing was managed by premixing a few percent of the water-soluble dopants with the water−gas mixture. The dopant is then expelled to the ice particle surface upon the crystallization of nanodroplets of the water−dopant solutions.[31] Isotopic exchange rates for such aerosols match closely those of array samples.

III. Results

Computational Results. Energy values of optimized slabs as a function of the position of OH^- in the system are shown in Figure 2. Each point in the plot is a result of a single geometry optimization; the results of 108 minimizations are presented.

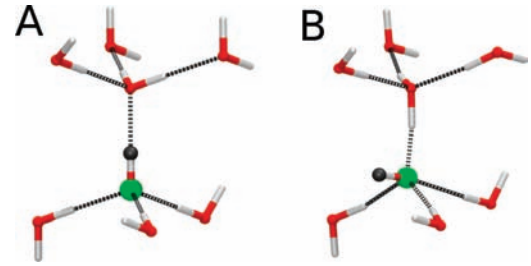

Figure 3. In-the-lattice (A) and off-the-lattice (B) type of OH^- structure inside Ih ice. For clarity, hydroxide with only seven nearest neighboring water molecules is presented. In (A), OH^- accepts three H-bonds and donates one H-bond; in (B), four H-bonds are accepted and none are donated. At the ice surface, in-the-lattice configurations are present in which OH^- points out of the surface; i.e., imagine configuration A without the top four water molecules.

In the simulation box, the z-axis was assumed to be perpendicular to the slab surfaces; therefore, the z-coordinate shows the position of hydroxide with respect to the surfaces. The z-values in a range of 0−2 Å correspond to OH^- placed at the sites located at the Fletcher-type surface (points in groups A and B in Figure 2), the range between 3 and 5 Å accounts for hydroxide located in the interior bilayer (group E), and the points with the z-coordinate above 6 Å describe slabs with hydroxide at the disordered surface (groups C and D). The red points correspond to in-the-lattice minima, while the blue points correspond to off-the-lattice minima. The geometries of the two types of interior minimum configurations are shown in Figure 3. It is noted that the final position of OH^- in a minimum does not necessarily correspond to its initial location, and that proton transfer was observed in the course of some of the minimizations.

Preliminary results on the internal OH^- minima were reported in a preceding study.[6] On the basis of ab initio dynamics simulations, it was proposed there that off-the-lattice internal configurations serve as traps for the hydroxide, because they inhibit proton transfer which is responsible for OH^- migration. On the other hand, if OH^- is located in the in-the-lattice configurations, proton transfer is feasible. In accord with this notion, all the initial off-the lattice configurations in the interior of the slab minimized to stable configurations with OH^- near the initial location. The energy range of the corresponding minima (blue points in group E of Figure 2), 7−16 kcal/mol, is remarkably broad. On the other hand, only about half of the minimizations with OH^- initially in internal in-the-lattice positions produced stable internal in-the-lattice minima (red points in group E); the latter minima span an energy range of 8−12 kcal/mol. The remaining minimizations of initially in-the-lattice internal configurations resulted in ejection of OH^- to the slab surface, via either one or a series of proton jumps. The average energy lowering as a result of the ejection was 9 kcal/mol (in the range 3−20 kcal/mol, energy lowering was estimated as the energy difference between the optimized surface location of OH^- and the very last minimization step in which OH^- was still in the interior bilayer). Considering the backward process, this quantity can be used as an estimate of an average cost of a first step of OH^- injection from the surface to the subsurface ice bilayer.

Minimizations of initially in-the-lattice configurations at the Fletcher surface resulted in a group of low-energy minima A, with the hydroxide embedded in a row of dangling-H atoms, at a three-coordinated surface site. At this site, the hydroxide ion accepts three H-bonds from the neighboring water molecules, the hydroxide hydrogen is unbound, and OH^- points out of the surface. The spread of energies in this group is quite narrow,

about 2.5 kcal/mol. In the two higher lying in-the-lattice minima (red points in group B), OH^- adopts a position at the four-coordinated half of the surface bilayer. A collection of off-the-lattice minima was also obtained at the four-coordinated sites of the Fletcher bilayer (blue points in group B), spanning an energy range of 4−7 kcal/mol. However, as explained in the Methods, generation of off-the-lattice minima is associated with converting one of the surface dangling-H atoms into a dangling O, which modifies the Fletcher structure and affects the energetics. Additional higher energy minima were found in group A of Figure 2 from minimization of initially off-the-lattice configurations in the surface bilayer, some of which converted to in-the-lattice ones in the course of the minimizations. However, in these minima the dangling-atom pattern was altered with respect to the Fletcher structure, and therefore, they were excluded from the plot for clarity. The different non-Fletcher surface configurations are discussed in connection with group D.

At the opposite proton-disordered surface, a fairly broad range of energies was obtained both for minima with hydroxide at three coordinated sites (group D in Figure 2) and for minima with OH^- at the four-coordinated sites (C). Blue points in group C correspond to off-the-lattice minima with OH^- localized at the inner half of the surface bilayer. The two red points in group C correspond to unusual in-the-lattice minima in which OH^- donates a bond to an inverted (originally three-coordinated) water molecule, with OH pointing into the slab.

However, the largest group of disordered surface minima corresponds to OH^- adopting three-coordinated positions with OH^- pointing out of the surface (group D, spanning an energy range of 0−9 kcal/mol). The input configurations of this group of minima included (i) in-the-lattice surface configurations, (ii) off-the-lattice surface configurations which converted to in-the-lattice ones in the course of the minimization (the latter subgroup includes the two lowest energy configurations in group D), and (iii) in-the-lattice interior configurations in which OH^- was evicted to the surface in the course of the minimization as noted above.

As shown in Figure 4, a hydroxide ion in group D is H-bonded to three four-coordinated water molecules within the surface, which are in turn bonded to six three-coordinated waters with either a dangling H or a dangling O. As indicated earlier, the energy of the slab is influenced both by the local arrangement of the dangling atoms around OH^- and by the global dangling-atom pattern at the two surfaces of the slab. In all minima in subgroups i and iii starting from in-the-lattice configurations, the global dangling-atom pattern is the same, so the influence on the energetics of the local arrangement of dangling atoms around OH^- can be elucidated. Within these subgroups we found configurations with 5−3 dangling-O atoms and 1−3 dangling-H atoms surrounding OH^- (Figure 4A−C). The configurations with 3 dangling-H atoms and 3 dangling-O atoms corresponded to an energy range of 3.3−4.5 kcal/mol. The configurations with 2 dangling-H atoms and 4 dangling-O atoms in the hydroxide neighborhood corresponded to an energy range of 5.1−6.6 kcal/mol. The configurations with 1 dangling-H atom and 5 dangling-O atoms corresponded to an energy range of 7.8−8.6 kcal/mol. Thus, the energy seems to decrease with increasing number of dangling-H atoms and decreasing number of dangling-O atoms in the neighborhood of the hydroxide.

An additional configuration with four dangling-H atoms/two dangling-O atoms near OH^- (as in Figure 4D) was generated "manually" from one of the configurations of type C in Figure 4, by exchanging the location of a more remote dangling H with one of the neighboring dangling-O atoms. The energy increased by 0.7 kcal/mol, suggesting that configurations with three dangling-H and three dangling-O neighbors (as in Figure 4C) are the most favorable. To further explore the issue, a set of auxiliary calculations was performed with an additional slab model of the same size but with a different orientational arrangement of H_2O which included a clump of dangling-H atoms at one of the surfaces. This model enabled a complementary investigation of configurations, in which the neighborhood of the surface hydroxide included 3−6 dangling-H atoms and 3−0 dangling-O atoms. The latter calculations confirmed that configurations with an equal number of dangling atoms of each kind in the hydroxide neighborhood are the most favorable. The energy of the system increased by up to ∼10 kcal/mol as the number of dangling-H atoms was increased with respect to this configuration and the number of dangling-O atoms was decreased.

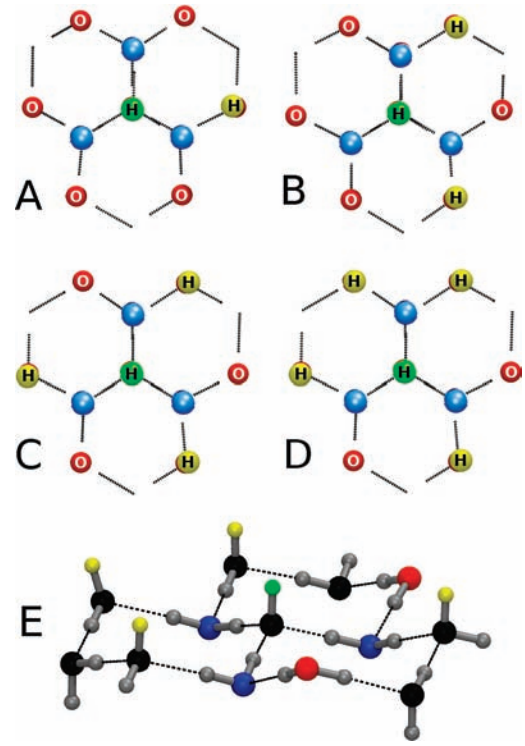

Figure 4. Schematic representations (A−D) of possible dangling-atom patterns in the proton-disordered surface in the neighborhood of the hydroxide. The hydroxide accepts hydrogen bonds from three neighboring four-coordinated water molecules, whose O atoms are marked blue. These molecules are in turn H-bonded to six three-coordinated water molecules with dangling atoms—either dangling O (marked red) or dangling H (marked yellow). Nondangling hydrogens are not presented. The number of dangling-H atoms of H_2O increases from (A) to (D); (C) appears to be the most stable structure with an alternating pattern of dangling-H and dangling-O atoms in the second neighborhood of OH^-. A fragment of the ice surface corresponding to configuration D is shown in (E) (nondangling oxygens are marked in black). See the text for more details.

Experimental Results. The H−D isotopic exchange for pure ice establishes a base rate for comparison with nanocrystals of ice coated to varying levels by adsorbates. The exchange rates induced by the addition/removal of the acid molecules H_2S and SO_2 were examined in an earlier study.[4] Protons released at the surface were observed to have an immediate impact on the exchange rates both at the surface and within the ice core with the rate enhancements significantly greater for SO_2 than H_2S. The base molecules, ammonia and MMA, have a surprising and more complex influence on the exchange at both the surface

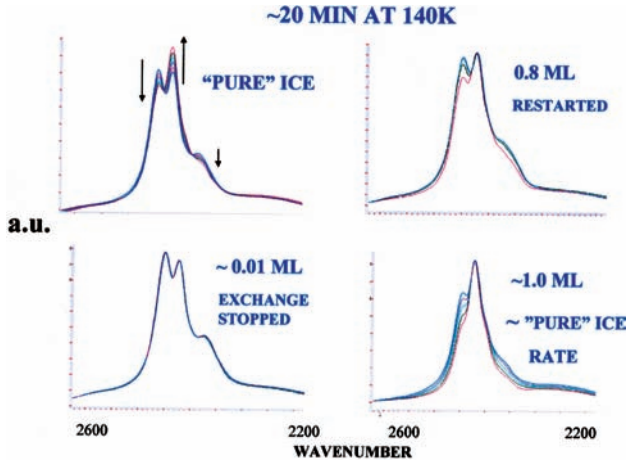

Figure 5. FTIR spectra showing the impact of isotopic exchange on the spectra of isolated D_2O in H_2O nanocrystals for a 20 min time period at 140 K with varying levels of adsorbed ammonia. The central HDO band increases as the D_2O side bands decrease with time except for the case of trace doping (i.e., ~0.01 ML). See the text for more details.

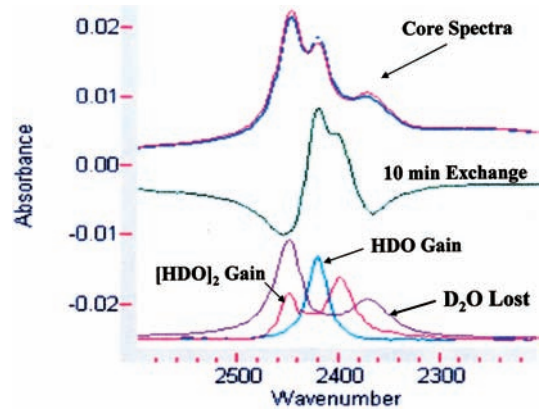

Figure 6. Details of the effect of 10 min of exchange at 136 K for a 90% ML ammonia-doped sample. The center curve indicates the overall change, while the bottom curves show (purple) the amount of lost D_2O, (red) the gain of $[HDO]_2$, and (turquoise) the gain of HDO. The absorbance scale is for the core spectra only, while other spectra have been enhanced by a factor of 10.

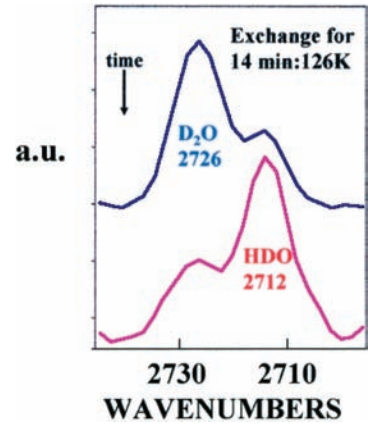

Figure 7. Surface dangling-OD bands of D_2O and HDO. The 14 cm^{-1} spacing between the HDO and D_2O frequencies enables the exchange rate measurements.

and the interior. The effect on the interior exchange over a 20 min period at 140 K is clear from Figure 5. The comparative results for pure ice nanocrystals, in the upper left quadrant, indicate extensive exchange as the central HDO band grows while the two D_2O bands fade. However, just a trace of ammonia, expected to release hydroxide ions through the reaction

$$NH_3 + H_2O \rightarrow NH_4^+ + OH^-$$

halts completely the interior exchange as shown in the lower left quadrant. Increasing the dosing of ammonia to 10% of a monolayer (ML) restarted the interior exchange, but at a barely detectable rate (not shown). The addition of near monolayer amounts of NH_3 returned the exchange rate to one approximating that of pure ice (as shown on the right side of Figure 5).

The spectra of Figure 5 show only the overall effects of isotopic exchange. However, as mentioned in section II, the spectra are a composite of absorption by three isolated deuterated isotopomers, namely, D_2O, $[HDO]_2$, and HDO, such that resolving the observed spectral changes with time into the three component spectra reveals the magnitude of both the proton and orientational defect activities.[18] An example resolution, using FTIR difference methods to show the details of exchange for nanocrystals of ice with 90% of an NH_3 ML for a 10 min period at 136 K, is given in Figure 6. The center curve indicates the overall change, while the three bottom spectra show the amount of lost D_2O, gain of $[HDO]_2$, and gain of HDO. A complete rate analysis requires recognition of the exchange sequence and the reversible nature of the deuteron hop and HDO turn steps,[18] but the about equal amounts of HDO and $[HDO]_2$ produced (Figure 6) indicate a somewhat faster turn than hop step.

Figure 7 shows an example of the nature of the FTIR spectra used to follow the isotopic exchange on the ice surface. The presence of dangling-D surface sites with different stretch frequencies for HDO vs D_2O is the point of emphasis. The spectra, separated by 14 min, show the rapid nature of the conversion of D_2O to HDO on the pure ice surface at 126 K, a temperature at which a few hours is required for a comparable level of exchange within the ice core (e.g., note the core exchange for pure ice at 140 K in Figure 5). Early studies on base adsorbates show that, as expected, NH_3 adsorbate molecules attach strongly to the dangling-H sites but, when isolated, tilt to the ice surface to gain significant added stability from multiple weak interactions.[32] Crowding, from an increased amount of adsorbate, promotes a more linear and significantly stronger H-bond to the surface dangling H, a factor that surely comes into play in the establishment of the surface OH^- population from base doping.

Nevertheless, even a trace of NH_3 or MMA dopant stops the surface isotopic exchange, as shown for MMA by the three top spectra of Figure 8. Here, a contrast is apparent with the bottom three spectra indicating exchange at the surface of pure ice at the same temperature (140 K) and for just half the time period. With a trace of MMA present, the intensity of the D_2O band at 2726 cm^{-1} is unchanged over an 8 min period, while for pure ice the D_2O half-life is <2 min. For several samples this base-induced kinetic stability of D_2O has been monitored for hours.

Trace amounts of ammonia also strongly inhibit surface as well as core exchange, and for both bases, a strong inhibition of surface exchange, relative to that of pure ice, extends beyond dopant levels required to restart the ice core exchange. Still, MMA does exhibit its greater base strength in other effects. The down-shift of the dangling-H frequency from association with MMA is greater by ~150 cm^{-1} with respect to that of ammonia (to ~2850 vs 3000 cm^{-1}), and the resumption of ice core isotopic exchange, which accompanies base doping beyond a few percent of a ML, is significantly more pronounced for

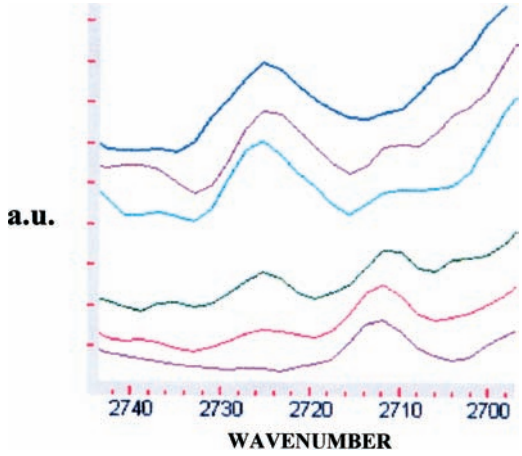

Figure 8. FTIR spectra comparing the surface H−D exchange at 140 K for ice nanocrystals with a trace of monomethylamine with that of pure ice. The top-down sequence of the top three spectra, with adsorbed MMA, is for 8 min, while the bottom three spectra for pure ice show the loss of D_2O intensity at 2726 cm^{-1} and gain of surface HDO intensity at 2712 cm^{-1} over a 4 min period. The half-life for surface exchange is increased from <2 min for the pure ice to a matter of hours by the trace of MMA.

MMA. Finally, there is some indication that ~1 ML of MMA leads to a significant infrared continuum that would correspond to the base analogue of the Zundel continuum[33] that has been observed for submonolayer amounts of HCl on the ice surface,[34] with the indication stronger for MMA than for ammonia. Such a continuum would signal incipient ionization induced by the MMA binding to the dangling hydrogens and reflect the greater base strength of MMA.

Semiquantitatively, NH_3-enabled ionic-defect activity has been observed to increase rapidly from near zero as the strongly base-doped samples were warmed near 130 K. The rapid rate increase extended to ~140 K, above which point the higher temperatures had a smaller impact. Such data indicate that the activation energy changes from a large value of ~12 kcal/mol to a more icelike value of ~8 kcal/mol,[18] hinting at a switch in the rate-controlling factor near 140 K.

IV. Summary, Discussion, and Conclusions

Computational DFT studies of the energetics of the hydroxide impurity within bulk ice and at the ice surface are reported. The calculations employed a three-bilayer crystal slab model containing 71 water molecules and 1 hydroxide ion. One side of the slab surface was fully "proton-disordered", while the other side corresponded to a so-called "Fletcher surface" [22,23] which included alternating rows of dangling-H and dangling-O atoms and which appears to be the ground state of the oxygen-ordered ice surface.

The hydroxide ion was placed at different crystal sites, and the structure was subjected to all-atom minimization. In the ice interior, two types of minima were calculated—in-the-lattice and off-the-lattice ones (Figure 3). The first type corresponds to a "textbook" model of hydroxide impurity in ice;[1] in this minimum, OH^- accepts three H-bonds and donates one. However, it was found that minimizations starting at about half of the interior in-the-lattice sites resulted in OH^- ejection to the surface via a sequence of (barrierless) proton jumps in the course of the minimizations. Off-the-lattice sites correspond to OH^- accepting four H-bonds and donating none; the OH^- axis points into a cavity in the ice structure. *Stable* off-the-lattice minima were located at each site of the interior bilayer of the model slab. The above results are consistent with a preliminary ab initio dynamics study[6] which indicated that proton transfer is inhibited in off-the-lattice configurations. The physical rationale is that the water configuration after proton transfer is unfavorable, with three acceptor H-bonds and one donor bond.

In classical proton-transfer models it is generally assumed that the energy of the ionic ice defect within the bulk does not vary significantly as a function of the defect location. The present results appear to contradict this assumption. The energy span of the interior in-the-lattice and off-the-lattice minima is 5 and 9 kcal/mol, respectively. (The energy span of in-the-lattice minima would be even broader if ejections to the surface in the course of some of the minimizations could be prevented, e.g., by the presence of adsorbate.) One may note that for about half of the stable interior in-the-lattice minima the energy of an off-the-lattice minimum is lower than that of the in-the-lattice one at the same site.

The calculated *surface* hydroxide minima include also two dominant types of configurations. Off-the-lattice configurations are localized at the four-coordinated sites in the inner half of the surface bilayer. In-the-lattice configurations correspond to OH^- localized at three-coordinated sites in the outer half of the surface bilayer; in these configurations, OH^- accepts three H-bonds from neighboring water molecules and points out of the surface. The energy of the latter configurations depends crucially on the arrangement of dangling atoms in the vicinity of the hydroxide (the dangling atoms nearest to OH^- belong to six second-nearest-neighbor water molecules; see Figure 4). A configuration with three dangling-H atoms and three dangling-O atoms in an alternating pattern around OH^- appears to be the most stable (Figure 4C). At the disordered surface, in-the-lattice minima with three-coordinated OH^- span a relatively broad energy range of 9 kcal/mol. At the Fletcher surface, the range is much narrower (~2.5 kcal/mol) because of the ordered dangling-atom pattern.

The present calculations show, that, on average, the energy of the surface OH^- sites is significantly lower than that of the interior ones. The surface preference, calculated as a difference between average energies of the bulk and the disordered surface minima, equals 5 kcal/mol. The average energy difference between the interior minima and the stable minima with three-coordinated OH^- at the Fletcher surface is 8 kcal/mol. This is in apparent contrast to liquid-phase simulations which do not indicate a significant surface preference for OH^-.[13,14] This difference between ice and liquid can be ascribed to the fact that, in contrast to liquid water, bulk ice is a very bad solvent of ions.[1]

The experimental part of this study focused on isotopic exchange in ice nanocrystals. The experiments rely on distinct spectroscopic signatures of D_2O, $(HDO)_2$, and HDO isotopic impurities isolated in H_2O ice. Conversion from D_2O to $(HDO)_2$ is used as a signature of proton transfer, while subsequent conversion to HDO is indicative of additional orientational defect activity. Here our main focus was on the first step. A small amount of basic adsorbate (ammonia or MMA) was shown to arrest both the bulk and the surface proton activity with respect to that of bare ice nanoparticles. Increasing base coverage was shown to restore the activity until, near monolayer coverage, it reached an extent similar to that of bare ice. In contrast, even weak acid adsorbates such as H_2S result in a monotonic increase in the exchange rate with respect to the bare nanoparticle value.[4]

For bare nanoparticles, the most likely source of ionic defects is water autoionization, which yields both hydroxide and hydronium ions (see Figure 9A). A small amount of base

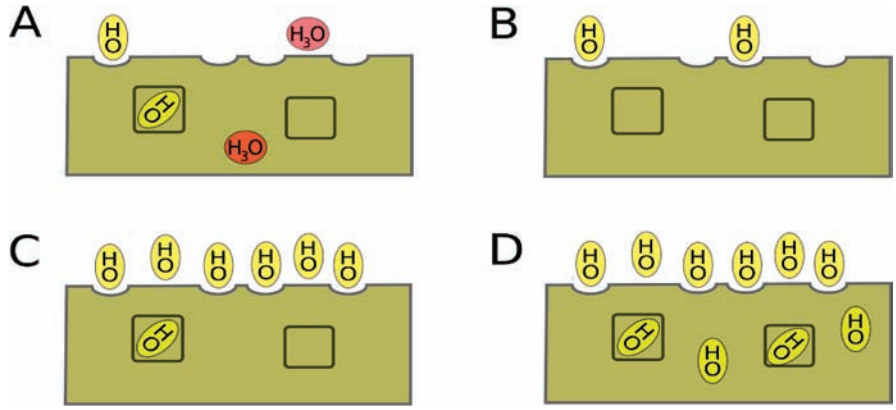

Figure 9. A schematic representation of the proposed scenario of ionic defect behavior in base-doped ice. (A) Bare nanoparticle (no ammonia adsorbed). Both hydronium and hydroxide are present due to water autoionization. Hydroxide is trapped by strongly binding sites (depicted as cavities at the surface and square-shaped sites in the interior). (B) Small ammonia coverage. Only hydroxide is present and is trapped by strongly binding surface sites. (C) Larger amount of ammonia. All strongly binding surface sites are occupied. Injection of OH^- to the ice interior occurs. Possible trapping of OH^- in strongly binding interior sites. (D) Highest amount of ammonia. Non strongly binding interior sites are populated.

adsorbate is expected to trap the protons, leaving some OH^- (see Figure 9B). The amount of OH^- is expected to increase with base coverage. The experimental results suggest that H_3O^+ is much more effective in inducing proton transfer within ice than OH^-. The present study is only informative on proton activity associated with the hydroxide (the hydronium will be addressed in a future study). We shall now attempt to interpret the experimental results using the computations.

It is noted first that the interpretation of the experimental results with the help of the computations is by no means straightforward. This is since the computational model assumed, for the sake of simplicity, a perfect crystal ice Ih structure, i.e., a periodic arrangement of O atoms of water (in conjunction with orientational disorder characteristic of ice Ih crystals). On the other hand, ice nanoparticles are known to adopt the cubic ice Ic structure.[30] Since the two crystal structures are closely related, we do not expect a qualitatively different behavior in ice Ic with respect to ice Ih. However, our past studies indicate that ice nanocrystals adopt a crystal structure only in the interior, while the surface is oxygen-disordered, and the subsurface partially disordered; the surface disordering appears to be associated with an increase in the surface concentration of fully four-coordinated water molecules (albeit with a strained coordination shell).[6,30] Moreover, the extent of surface and subsurface disordering is affected by H-bonding adsorbates, which cleave some of the strained surface H-bonds. In an oxygen-disordered surface, formation of ordered rows of dangling atoms is not possible; thus, the present computational results for a proton-disordered surface seem more relevant to the experimental conditions than for the Fletcher surface. The energy range of the hydroxide binding sites is expected to be even broader in the case of the experimental surfaces than in the computational model because of the additional oxygen disorder.

The very low proton activity observed experimentally at low base coverage can be then ascribed to the fact that, at low concentration, OH^- ions become trapped at the most stable surface sites with a favorable arrangement of neighboring dangling atoms (as shown in Figure 9A). Surface restructuring induced by the adsorbed OH^- ions to create low-energy traps is likely due to enhanced rotational freedom of water molecules at the surface; this would additionally contribute to OH^- immobilization at the surface, hindering the surface mobility of protons. It should also be also noted that there are additional factors that may impede proton mobility in ice in the presence of the hydroxide which were not included in the present computational study. The role of the cation formed in the base ionization reaction (NH_4^+ in the case of ammonia) should be considered. These cations are expected to be relatively immobile, and ion pair creation with anions and thus further contribution to immobilization of hydroxide cannot be excluded.

Increasing base coverage is expected to affect the proton activity in several ways. The most obvious one is an increasing number of hydroxide ions. The second is involvement of dangling-H atoms at the surface in bonding with ammonia or MMA adsorbate. The corresponding H-bonds are very strong (as evidenced, e.g., by 700 and 800 cm^{-1} frequency shifts of the OH^- stretch upon bonding with ammonia and MMA adsorbates). Dangling-H sites bonded to the adsorbate are expected to be much less favorable for the hydroxide than the bare ones because of repulsion from the partial negative charge on the nitrogen, thus impeding hydroxide eviction from the bulk to the surface. This expectation was further tested by us using the following computation: The proton-disordered surface of the slab model was covered by five ammonia molecules, so that each dangling-H atom was bonded to one adsorbate NH_3. The hydroxide ion was then placed at an internal in-the-lattice site, such that ion eviction to the surface took place in the course of the previous minimization of the slab with a bare surface (the eviction occurred to the proton-disordered surface by two proton-transfer events). In the case of an ammonia-covered surface, such an eviction did *not* happen, and a stable minimum was obtained with OH^- located at the initial in-the-lattice site. By making surface sites less favorable, the presence of base adsorbate should then facilitate injection of hydroxide to the ice interior (see Figure 9C). (An analogous result was obtained recently[5] in the context of SO_2 ionization at the surface of ice; it was found there that dangling-O sites bonded to SO_2 adsorbate are unfavorable for the hydronium in contrast to the bare ones.)

The experimentally observed increase in proton activity with base coverage is proposed to be associated with (a) saturation of the deepest OH^- binding sites at the surface, (b) making the surface less attractive to OH^- since the favorable dangling-H sites are largely occupied by the adsorbate, and (c) impeding relaxation of the dangling-atom pattern around the surface OH^-, since the adsorbate is strongly bonded to dangling-H sites. The limited proton activity observed even at the highest base coverage (at which it is comparable to that of bare ice) may be associated with trapping of hydroxide ions at off-the-lattice sites, at which proton transfer is impeded (see Figure 9D).

The experimentally measured activation energy for isotopic exchange, ~10 kcal/mol, should include several contributions—from the reaction $NH_3 + H_2O \rightarrow NH_4^+ + OH^-$, from the anion overcoming the attraction to the (surface) cation, from the injection of the proton to the interior, and from proton jumps between hydroxide sites of unequal energy. It appears that the last two contributions dominate the activation energy, since their size is on the order of the calculated energy span of the hydroxide sites. The contribution of the reaction $NH_3 + H_2O \rightarrow NH_4^+ + OH^-$ is of some interest; it is expected to be endothermic on the basis of the thermochemical data for an aqueous solution. While the reaction enthalpy at cold ice surfaces is expected to differ from that of a room temperature solution, the qualitative expectation of the endothermicity is supported by the spectroscopic observation that most of the base adsorbate is un-ionized. Due to the endothermicity, at high base coverage one expects an increasing number of hydroxide ions with increasing temperature. This increase may be associated with the observed reduction in the effective activation energy for the isotopic exchange from ~12 to ~8 kcal/mol as the temperature increases. This is since a larger number of hydroxide ions results in better saturation of the deep trap sites.

There are still many open questions associated with proton transfer in ice. Perhaps the most intriguing question is why proton transfer is so much more effective in acid-doped samples than in base-doped ones; work is in progress on a hydronium-doped ice slab.

Acknowledgment. Funding by ISF, NSF, and BSF grants is gratefully acknowledged.

References and Notes

(1) Petrenko, V. F.; Whitworth, R. W. *Physics of Ice*; Oxford University Press: Oxford, U.K., 1999.
(2) Bjerrum, N. *Science* **1952**, *115*, 385–390.
(3) Uras-Aytemiz, N.; Joyce, C.; Devlin, J. P. *J. Chem. Phys.* **2001**, *115*, 9835–9842.
(4) Devlin, J. P.; Buch, V. *J. Chem. Phys.* **2007**, *127*, 91101.
(5) Jagoda-Cwiklik, B.; Buch, V. *Phys. Chem. Chem. Phys.* **2008**, *10*, 4678.
(6) Cwiklik, L.; Buch, V. *Phys. Chem. Chem. Phys.* **2009**, *11*, 1294–1296.
(7) CP2K version 2.0.0, 2008. http://cp2k.berlios.de/.
(8) Krack, M.; Mohamed, F.; Parrinello, M.; Chassaing, T.; Hutter, J. *Comput. Phys. Commun.* **2005**, *167*, 103–128.
(9) Knight, C.; Singer, S. J. Theoretical study of a hydroxide ion within the ice-Ih lattice. In *Physics and Chemistry of Ice*; Kuhs, W. F., Ed.; Royal Society of Chemistry: London, 2007; pp 339–346.
(10) Tuckerman, M.; Chandra, A.; Marx, D. *Acc. Chem. Res.* **2006**, *39*, 151–158.
(11) Megyes, T.; Balint, S.; Grosz, T.; Radnai, T.; Bako, I. *J. Chem. Phys.* **2008**, *128*, 044501.
(12) Aziz, E. F.; Ottosson, N.; Faubel, M.; Hertel, I. V.; Winter, B. *Nature (London)* **2008**, *455*, 89–91.
(13) Buch, V.; Milet, A.; Vacha, R.; Jungwirth, P.; Devlin, J. P. *Proc. Natl. Acad. Sci. U.S.A.* **2007**, *104*, 7342–7347.
(14) Vacha, R.; Buch, V.; Milet, A.; Devlin, J. P.; Jungwirth, P. *Phys. Chem. Chem. Phys.* **2007**, *9*, 4736–4747.
(15) Petersen, P.; Saykally, R. *Chem. Phys. Lett.* **2008**, *458*, 255–261.
(16) Beattie, J. K. *Phys. Chem. Chem. Phys.* **2008**, *10*, 330–331.
(17) Vacha, R.; Buch, V.; Milet, A.; Devlin, J. P.; Jungwirth, P. *Phys. Chem. Chem. Phys.* **2008**, *10*, 332–333.
(18) Collier, W. B.; Ritzhaupt, G.; Devlin, J. P. *J. Phys. Chem.* **1984**, *88*, 363.
(19) Wooldridge, P. J.; Devlin, J. P. *J. Chem. Phys.* **1988**, *88*, 3086.
(20) Devlin, J. P. *J. Chem. Phys.* **2000**, *112*, 5527–5529.
(21) Lee, C.-W.; Lee, P.-R.; Kang, H. *Angew. Chem., Int. Ed.* **2006**, *45*, 5529–5533.
(22) Fletcher, N. H. *Philos. Mag. B* **1992**, *66*, 109–115.
(23) Buch, V.; Groenzin, H.; Li, I.; Shultz, M. J.; Tosatti, E. *Proc. Natl. Acad. Sci. U.S.A.* **2008**, *105*, 5969–5974.
(24) Pan, D.; Liu, L.-M.; Tribello, G. A.; Slater, B.; Michaelides, A.; Wang, E. *Phys. Rev. Lett.* **2008**, *101*, 155703.
(25) Buch, V.; Sandler, P.; Sadlej, J. *J. Phys. Chem. B* **1998**, *102*, 8641–8653.
(26) McDonald, S.; Ojamae, L.; Singer, S. J. *J. Phys. Chem. A* **1998**, *102*, 2824–2832.
(27) Becke, A. D. *Phys. Rev. A* **1988**, *38*, 3098–3100.
(28) Lee, C. T.; Yang, W. T.; Parr, R. G. *Phys. Rev. B* **1988**, *37*, 785–789.
(29) Goedecker, S.; Teter, M.; Hutter, J. *Phys. Rev. B* **1996**, *54*, 1703–1710.
(30) Buch, V.; Bauerecker, S.; Devlin, J. P.; Buck, U.; Kazimirski, J. K. *Int. Rev. Phys. Chem.* **2004**, *23*, 375–433.
(31) Hernandez, J.; Uras, N.; Devlin, J. P. *J. Phys. Chem. B* **1998**, *102*, 4526–4535.
(32) Delzeit, L.; Powell, K.; Uras, N.; Devlin, J. P. *J. Phys. Chem. B* **1997**, *101*, 2327–2332.
(33) Zundel, G. *Adv. Chem. Phys.* **1983**, *111*, 1–217.
(34) Devlin, J. P.; Uras, N.; Sadlej, J.; Buch, V. *Nature (London)* **2002**, *417*, 269–271.

JP900545D